Ab initio molecular-dynamics study of the structural and transport properties of liquid germanium

R. V. Kulkarni, W. G. Aulbur, and D. Stroud

Department of Physics, The Ohio State University, Columbus, Ohio 43210

(Received 23 September 1996)

We describe the results of *ab initio* molecular-dynamics simulations of liquid Ge at five temperatures ranging from 1250 to 2000 K. The electronic structure is calculated using the local-density approximation and generalized norm-conserving pseudopotentials. The calculations yield the pair correlation function, the static structure factor, the bond-angle distribution function, the electronic density of states, the atomic self-diffusion coefficient, and finally the ac conductivity. Near melting, the structure factor has the experimentally observed shoulder on the high-k side of the principal peak, which becomes progressively less distinct at higher temperatures. The bond-angle distribution function indicates the persistence of covalent bonding for shorter bond lengths in the liquid state. The electronic density of states is metallic at all the temperatures with a pseudogap at a binding energy of 4.6 eV. The diffusion constant shows a sharp rise between 1250 and 1500 K (1.2×10^{-4}–2.0×10^{-4} cm^2 s^{-1}) and increases less rapidly at higher temperatures, to only 2.3×10^{-4} cm^2 s^{-1} at 2000 K. [S0163-1829(97)02711-2]

I. INTRODUCTION

Liquid Ge (*l*-Ge) has a number of unusual properties, which have prompted several experimental and theoretical studies. In the crystalline phase, Ge is a diamond-structure semiconductor with a direct band gap of about 0.9 eV. Upon melting, Ge undergoes a semiconductor-metal transition accompanied by significant structural changes. The density increases by about 4.7%, and its coordination number, as determined by x-ray diffraction,[1] grows from 4 in the solid phase to about 6.8 in the liquid. Similarly, the electrical conductivity increases on melting by more than an order of magnitude, to about 1.6×10^{-4} Ω^{-1} cm^{-1},[2] a range characteristic of metallic behavior.

Despite its metallic nature, however, the behavior of *l*-Ge is more complicated than that of a simple liquid metal. Simple liquid metals usually have structure factors similar to that of a fluid of hard spheres, with a temperature-dependent packing fraction and a coordination number of about $10-12$.[3] Apart from having a lower coordination number, *l*-Ge also has a structure factor with a shoulder on the high-k side of the first peak, a feature that cannot be reproduced by a hard-sphere model. These differences have been interpreted as indications that covalent bonding persists in the liquid state.[2] This interplay between metallic and covalent bonding makes *l*-Ge of particular theoretical interest.

The properties of liquid semiconductors are also important from a technological point of view. Since most semiconductors are grown from the melt, the transport coefficients of the liquid, such as the diffusion constant, are needed as input in the fluid-dynamic equations used to model crystal growth. However, these properties are difficult to determine experimentally. Typical experiments to measure such diffusion constants are based on tracer diffusion through capillary tubes.[4] Such experiments suffer from uncertainties arising from the contributions of convection and of gravity. These uncertainties can be overcome, in principle, by carrying out the experiments in microgravity.

On the theoretical side, most numerical studies of *l*-Ge have been carried out using molecular-dynamics simulations. One approach is to obtain the interatomic forces using empirical potentials that include three-body terms to model the covalent contributions. While such simulations[5,6] can reproduce the observed structure factors for liquid semiconductors, they tend to overestimate the degree of tetrahedral bonding in the liquid state. Also, the empirical potentials used are independent of both density and temperature, whereas the actual many-body potential for *l*-Ge depends on both.

An alternative approach is to derive the interatomic forces by expanding the total energy to second order in the electron-ion pseudopotential, using the linear-response function of the electron gas.[7] The pair correlation function and structure factor obtained from this method agree fairly well with experiment. But this method omits the many-body contributions to interatomic forces, which are important in *l*-Ge. Thus, to understand the effects of covalent bonding in *l*-Ge, one must treat the interatomic forces at a level beyond second-order perturbation theory.

Since the pioneering work of Car and Parrinello,[8] several molecular-dynamics schemes have been developed that treat the interatomic forces in a microscopic, fully quantum-mechanical manner. The feature common to all is that the electronic degrees of freedom are treated quantum mechanically to determine the forces on the ions, after which the ionic motion itself is handled using classical dynamics. This approach, usually called *ab initio* molecular dynamics, has recently been applied by several groups to study liquid semiconductors, including *l*-Ge.[9–11] Most of these studies, however, have emphasized the properties at only one temperature in the liquid state and thus omit possibly important temperature-dependent changes in the atomic and the electronic structure.

In this paper we carry out *ab initio* simulations for liquid

Ge at *five* temperatures ranging from 1250 to 2000 K, thereby obtaining information about the temperature dependence of various observables in the liquid state. At each temperature, we study a range of structural, electronic, and atomic properties of liquid Ge. Among these are the electronic density of states, the static structure factor, the atomic self-diffusion diffusion coefficient, and the dc and ac conductivities. Our simulations are carried out over a time interval of more than 1.5 ps at each temperature.

Besides considering several temperatures, our simulations also differ from previous work in various technical details. In particular, we avoid treating Fourier coefficients of electronic wave functions as fictitious dynamical variables, as is done in the Car-Parrinello approach, and, in order to converge the electronic structure at each step, we use the so-called Williams-Soler algorithm instead of the conjugate-gradient approach.

The rest of our paper is organized as follows. In Sec. II we discuss the method and computational details. Our results are presented in Sec. III. Section IV describes our results and gives some conclusions.

II. METHOD AND COMPUTATIONAL DETAILS

A. Method

Our simulation method proceeds as follows. First, for a fixed ionic configuration, the electronic structure is converged to the Born-Oppenheimer surface, that is, the equilibrium electronic state is determined for the instantaneous ionic configuration. Next, the forces on the ions are calculated using the Hellmann-Feynman theorem and the ions are moved according to these forces. For the new ionic coordinates the electronic structure is again recalculated and converged to the Born-Oppenheimer surface and this procedure is repeated for the duration of the simulation.

In calculating the electronic structure we use the finite-temperature version of electron density-functional theory and the electronic subsystem is assumed to be at a fictitious temperature T^{el}. Thus the variational quantity to be minimized, for a fixed configuration of the ions, is the free-energy functional. Let f_i be the occupation number of the ith single-particle state ψ_i. Then the free-energy functional is given by

$$F[\{\psi_i(r)\},\{f_i\}] = E[\{\psi_i(r)\},\{f_i\}] - T^{el}S^{el}[\{f_i\}], \quad (1)$$

where $S^{el}[\{f_i\}]$ is the electronic entropy, given by

$$S^{el}[\{f_i\}] = -2k_B \sum_i [f_i \ln f_i + (1-f_i)\ln(1-f_i)]. \quad (2)$$

With this choice for $S^{el}[\{f_i\}]$, minimizing the free-energy functional with respect to the occupation numbers yields the Fermi-Dirac distribution

$$f_i = \left[\exp\left(\frac{\varepsilon_i - \mu}{k_B T^{el}} \right) + 1 \right]^{-1}, \quad (3)$$

ε_i being the corresponding Kohn-Sham eigenvalue and μ the chemical potential. This finite-temperature procedure is necessary to avoid numerical problems in the simulation arising from discontinuous changes in the occupation numbers.[12]

TABLE I. Lattice constant a_{lat}, bulk modulus B, and binding energy per atom E_B for diamond-structure Ge at temperature $T = 0$, as calculated in the present work and as obtained experimentally (quoted by Ref. 9).

Property	Calculated	Experiment
a_{lat} (bohrs)	10.63	10.68
B (GPa)	69.4	76.5
E_B (eV)	5.01	3.85

The minimization of the free-energy functional with respect to variations in the single-particle wave functions ψ_i leads to the Kohn-Sham equations.[13] The actual minimization is carried out by expanding the single-particle wave functions in plane waves and using the Williams-Soler algorithm.[14] Once the single-particle wave functions are self-consistently determined, the force on the ith ion is computed using the Hellmann-Feynman theorem. A detailed description of the molecular-dynamics code used in the calculations can be found in the literature.[15,16]

B. Computational details

We carry out the electronic-structure calculations in the local-density approximation (LDA), together with the Ceperley-Alder exchange-correlation functional as parametrized by Perdew and Zunger.[17] We use generalized norm conserving pseudopotentials[18] in the Kleinman-Bylander form,[19] choosing the d-wave part of the pseudopotential as the local component. We take the $4s$ and $4p$ states of Ge as the valence states and we apply non-linear core-valence corrections.[20] To check this pseudopotential, we determined the ground-state properties of crystalline Ge, using an energy cutoff of 20 Ry and a set of six k points in the irreducible wedge of the Brillouin zone. The resulting zero-temperature lattice constant, bulk modulus, and binding energy of Ge are in reasonably good agreement with experiment (cf. Table I). (The binding energy is somewhat larger than experiment, as is characteristic of LDA calculations.)

To generate the initial configurations in the liquid state, we use a classical molecular-dynamics code[21] based on empirical potentials of the Stillinger-Weber form.[5] Our simulations are carried out in a 64-atom supercell with simple cubic periodic boundary conditions. Note that such a cell size is commensurate with a possible diamond-structure ground state. The densities for the different temperatures are chosen to match published experimental data.[2] The plane-wave energy cutoff in the liquid state is 10 Ry, and we use Γ-point sampling for the supercell Brillouin-zone integration. The ionic equations of motion are integrated by means of the Verlet algorithm, using an ionic time step of 125 a.u. ($\sim$3 fs). The ionic temperature is controlled by means of the Nosé-Hoover thermostat,[22,23] using a thermostat mass parameter Q of about 1×10^6 a.u. The fictitious temperature for the electronic subsystem is $k_B T^{el} = 0.1$ eV and we calculate the electronic wave functions for the lowest 134 bands, i.e., including six empty bands.

Using this approach, we converge the total energy until the change in the energy in successive steps falls below 5×10^{-6} eV/atom. Since our starting ionic configurations are
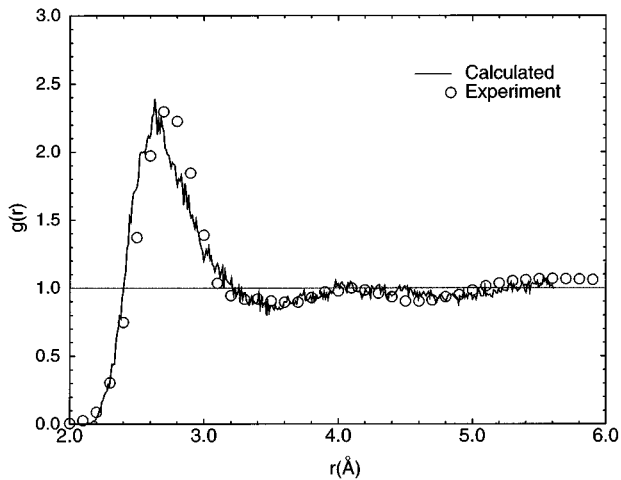
FIG. 1. Pair correlation function $g(r)$ for liquid Ge at $T = 1250$ K. Dashed lines, calculated $g(r)$ as obtained from present simulations; circles, experiment (Ref. 1).

already close to equilibrium at the temperature considered, we find that simulations of only 1.5 ps are adequate to extract the self-diffusion coefficients at these temperatures.

III. RESULTS

A. Structural properties

We begin by describing our results for the pair correlation function $g(r)$. Figures 1 and 2 show $g(r)$ at the temperatures $T = 1250$ and 2000 K. As can be seen from Fig. 1, the results agree with experiment. At this temperature, the principal peak in the calculated $g(r)$ occurs at $r = 2.63$ Å, in good agreement with the experimental values of 2.70 and 2.66 Å.[1,24] An effective coordination number N_c can be obtained by integrating $n \times 4\pi r^2 g(r)$ from $r = 0$ to the first minimum r_m, where n is the number density. If we choose r_m to be 3.2 Å, which is the experimentally observed value for the first minimum, we get $N_c = 6.0$. In our simulation, however, the first minimum falls between 3.35 and 3.45 Å. If we therefore choose as a cutoff $r_m = 3.4$ Å, we obtain $N_c = 7.1$. Clearly, N_c is rather sensitive to the choice of r_m, a quantity that is not sharply defined for liquid Ge. Bearing this ambiguity in
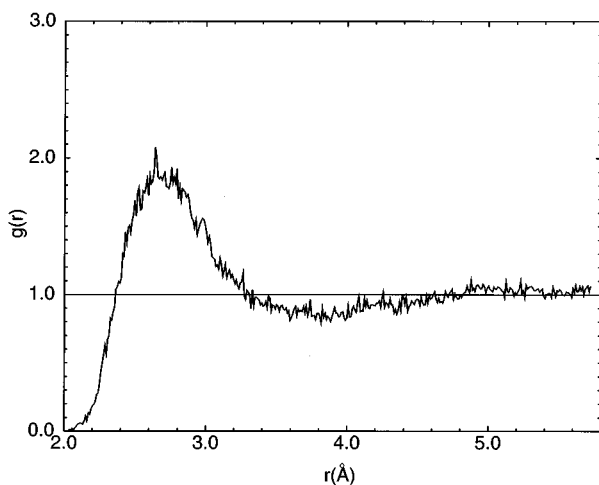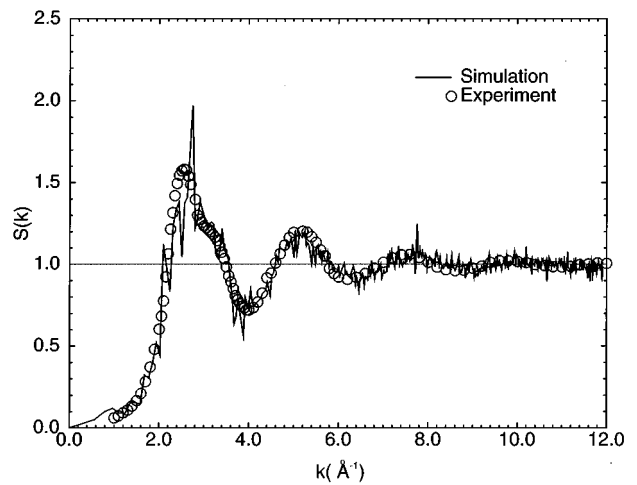

FIG. 3. Static structure factor $S(k)$ as a function of wave vector k (in Å^{-1}) for liquid Ge at $T = 1250$ K. Dashed lines, present calculations; circles, experiment (Ref. 1).

mind, we can still see that both r_m and N_c grow with increasing T. At $T = 2000$ K, for example, using $r_m = 3.6$ Å, we obtain a coordination number of $N_c = 8.0$. By comparison, N_c is 4 in diamond-structure Ge, 12 in a close-packed solid, and about 10 in a typical hard-sphere liquid.

At $T = 1250$ K, $g(r)$ has a weak intermediate peak at $r = 4.1$ Å lying between the two principal peaks. This peak flattens with increasing T, disappearing completely at $T = 2000$ K (cf. Fig. 2). The height of the first peak of $g(r)$ also diminishes with increasing T, but occurs at roughly the same r, which is in good agreement with experiments done by Filipponi and DiCicco.[25]

Figures 3 and 4 show the calculated static structure factor $S(k)$ for the same temperatures. $S(k)$ is defined by the relation

$$S(k) = \frac{1}{N}\langle \rho_{\mathbf{k}} \rho_{-\mathbf{k}} \rangle - N \delta_{\mathbf{k},0}. \qquad (4)$$

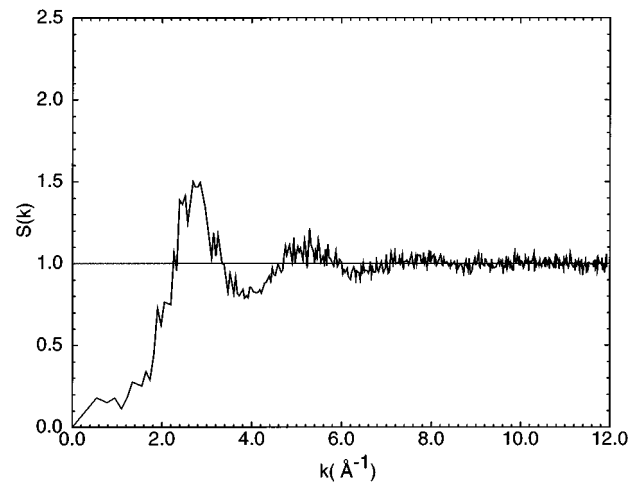Here $\rho_{\mathbf{k}}$ is a Fourier component of the atomic density, defined by

FIG. 2. Calculated $g(r)$ for $T = 2000$ K.

FIG. 4. Calculated $S(k)$ for $T = 2000$ K.

TABLE II. Structure factor $S(0) \equiv \lim_{k \to 0} S(k)$ (see text), ionic number density n, and height of the principal peak in $g(r)$, calculated at five temperatures.

T (K)	$S(0)$	n (Å^{-3})	$g(r_{max})$
1250	0.05	0.04526	2.39
1400	0.11	0.04457	2.23
1500	0.12	0.04413	2.13
1600	0.12	0.04370	2.08
2000	0.18	0.04250	2.00

$$\rho(\mathbf{k}) = \sum_n e^{-i\mathbf{k} \cdot \mathbf{R}_n}, \qquad (5)$$

where $\mathbf{R}_n$ is the position of the nth atom and N is total number of atoms. In calculating $S(k)$, we average over the last 450 simulation time steps and also over all $\mathbf{k}$ vectors of equal magnitude.

At the lowest temperatures, our calculated $S(k)$ shows the characteristic feature of the structure factor for liquid Ge observed in neutron diffraction studies: a distinct shoulder on the high-k side of the principal peak that occurs at $k = 3.45$ Å^{-1}. The results are in excellent agreement with the measured $S(k)$ at $T = 1250$ K. As T increases, the principal peak is reduced in height and the shoulder becomes less distinct. By $T = 2000$ K, the shoulder has completely disappeared (cf. Fig. 4) and the structure factor resembles that of a simple liquid metal well above melting.

As T increases, our calculations also predict an increase in small-angle x-ray or neutron scattering, as measured by $\lim_{k \to 0} S(k)$. In turn, $S(0)$ is related to the isothermal compressibility χ_T by the compressibility sum rule

$$\lim_{\mathbf{k} \to 0} S(\mathbf{k}) = S(0) = n k_B T \chi_T, \qquad (6)$$

where n is the ionic number density. Now Egelstaff *et al.*[26] have shown that in practice, for liquid metals, $S(0) \approx S(k_1/4)$, where k_1 corresponds to the principal peak of $S(k)$. Using this estimate, we can calculate the isothermal compressibility of l-Ge at $T = 1250$ K as $\chi_T = 6.4 \times 10^{-11}$ m^2 N^{-1}. Table II lists the calculated $S(0)$'s, as obtained from the Egelstaff estimate, along with the corresponding $n(T)$ and the height of the first peak in $g(r)$.

More information about the structural properties can be obtained from the *bond angle distribution function* $g^{(3)}(\theta, r_c)$. $g^{(3)}$ gives the distribution of the angle formed by pairs of vectors drawn from a reference atom to any two other atoms within a cutoff radius r_c of that atom. Figures 5 and 6 show $g^{(3)}(\theta, r_c)$ for $T = 1250$ and 2000 K. If r_c is chosen as the first minimum in $g(r)$, $g^{(3)}(\theta, r_c)$ shows two peaks at $T = 1250$ K: one at $\theta \sim 60°$ and a second broader peak centered at 98°. If instead $r_c = 2.8$ Å (roughly equal to the covalent bond length in crystalline Ge), the 60° peak disappears while that near 98° persists.

As T increases, we observe several changes in $g^{(3)}(\theta, r_c)$. (a) For the larger cutoff radius r_c, the 60° peak becomes slightly more pronounced, while that at $\sim$98° becomes slightly less so. (b) For the smaller cutoff radius
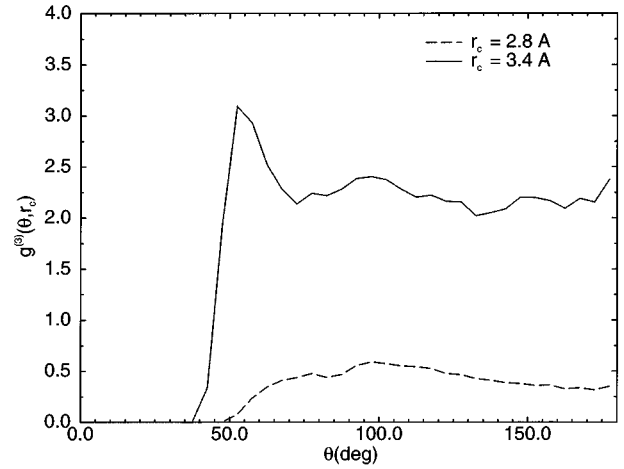

FIG. 5. Calculated bond angle distribution function $g^3(\theta, r_c)$ for liquid Ge at $T = 1250$ K for $r_c = 2.8$ and 3.4 Å.

($r_c = 2.8$ Å), there is a change from a single broad peak near 98° at $T = 1250$ K to an almost uniform distribution in the bond angles at $T = 2000$ K, slightly peaked near 60°. The 98° peak suggests a ''flattened'' tetrahedral arrangement of the atoms, similar to the so-called β-tin structure,[27] whereas that at 60° is typical of metallic bonding and represents a more closely packed structure. In short, the structure gradually changes from an open structure, with tetrahedral bonding for shorter bond lengths, just above melting, to a more closely packed structure with very little tetrahedral bonding at very high temperatures ($T = 2000$ K).

B. Atomic self-diffusion

We now turn to our results for the atomic self-diffusion coefficient $D(T)$ in liquid Ge. To study $D(T)$, we first follow the time-dependent mean-square ionic displacement in the liquid. We start from the equilibrium liquid configuration generated by classical molecular dynamics. For sufficiently long time intervals, $D(T)$ can be extracted from the equation

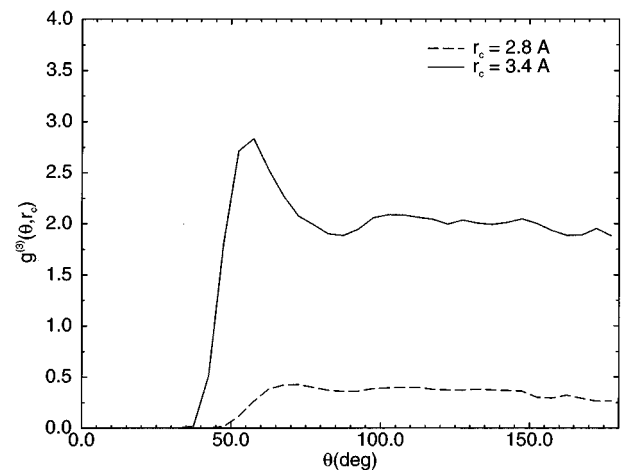$$D(T) = \lim_{t \to \infty} \frac{\langle |\mathbf{R}_I(t) - \mathbf{R}_I(0)|^2 \rangle}{6t}, \qquad (7)$$
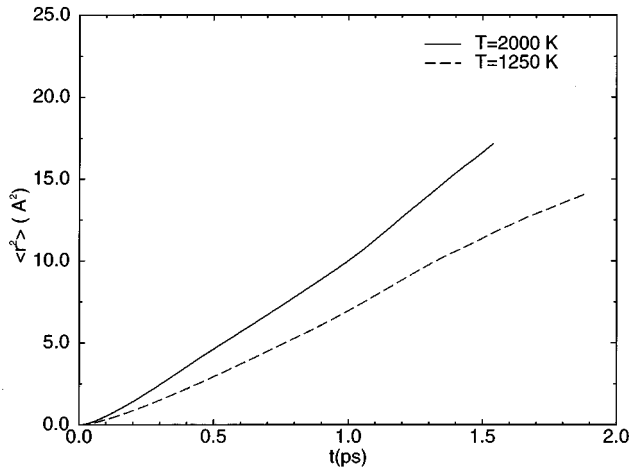

FIG. 6. Same as Fig. 5, but for $T = 2000$ K.

FIG. 7. Mean-square atomic displacements $\langle r^2 \rangle \equiv \langle |\mathbf{R}_I(t) - \mathbf{R}_I(0)|^2 \rangle$ (in Å^2) versus time t (in ps), calculated at $T = 1250$ K and $T = 2000$ K.

where $\mathbf{R}_I(t)$ denotes an ionic position at time t. The angular brackets denote an average over all the ions and also over all time origins. In our calculations we have computed the average, taking the beginning of each time step as a different time origin.

Our calculated mean-square displacements are shown in Fig. 7 for two representative temperatures: $T = 1250$ and 2000 K. $D(T)$ is obtained from a linear-regression fit of the last 0.6 ps of data to a straight line. Table III shows the resulting $D(T)$ for all temperatures considered, along with the experimental results of Pavlov and Dobrokhotov[28] and results from previous *ab initio* and empirical simulations. As expected, $D(T)$ is a monotonically increasing function. Our results agree well with experiment and also with the *ab initio* calculations of Kresse and Hafner for $T = 1250$ K,[9] but at the other temperatures are somewhat higher than other *ab initio* predictions.[10,11] Possibly some of these differences arise from the fact that the densities chosen in the various simulations are different. Previous calculations at elevated temperatures have used the density of liquid Ge at melting, whereas we choose a lower density appropriate to the temperature,

TABLE III. Calculated and measured atomic self-diffusion coefficients $D(T)$.

T (K)	$D(T)$ (10^{-4} cm^2/s)	$D(T)$ (other calculations)	$D(T)$ (experiment)
1250	1.2[a]	1.0[b], 0.44[c]	1.21, 0.78[f]
1400	1.7[a]	1.0[d]	1.62[f]
1500	2.0[a]	1.2[e]	3.21[f]
1600	2.1[a]		
2000	2.3[a]		

[a]Results of the present calculations, carried out by *ab initio* molecular dynamics at five temperatures.
[b]Kresse and Hafner (Ref. 9) (at $T = 1230$ K).
[c]Yu *et al.* (Ref. 21) (empirical potential).
[d]Godlevsky *et al.* (Ref. 11) (at $T = 1350$).
[e]Takeuchi and Garzón (Ref. 10).
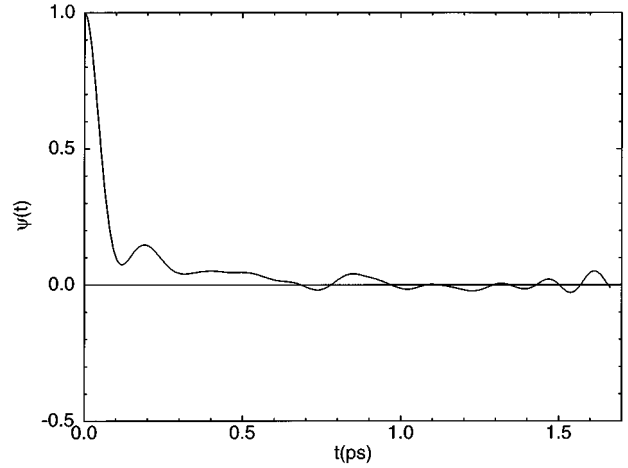[f]P. V. Pavlov and E. V. Dobrokhotov (Ref. 28).

FIG. 8. Velocity autocorrelation function $\psi(t)$ as defined in the text, plotted versus time t (in ps), at $T = 1250$ K.

determined from experiment.[2] In addition, of course, each of the simulations uses a slightly different *ab initio* method.

$D(T)$ may also be obtained from the velocity autocorrelation function $\psi(t)$, defined by

$$\psi(t) = \frac{\langle \mathbf{v}_i(t) \cdot \mathbf{v}_i(0) \rangle}{\langle \mathbf{v}_i(0) \cdot \mathbf{v}_i(0) \rangle}. \tag{8}$$

Here the angular brackets again denote an average over all the atoms and over different time origins. The diffusion constant D is then obtained from the relation

$$D = \frac{k_B T}{M} \int_0^\infty \psi(t) dt. \tag{9}$$

A representative plot of $\psi(t)$ $T = 1250$ K is shown in Fig. 8. The resulting $D(T)$ agrees to within 5–10 % with the values extracted from the mean-square displacement; both are shown in Fig. 9.
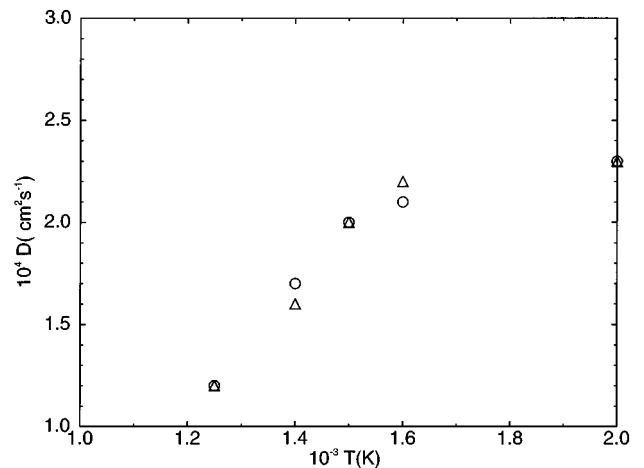

FIG. 9. Calculated diffusion constant $D(T)$ (in cm^2/s) versus temperature T. Points denoted $\bigcirc$ are obtained using the mean-square displacement, those denoted $\triangle$ from the velocity autocorrelation function.

A notable feature of our results is that the diffusion constant rises sharply between $T = 1250$ and 1500 K and more slowly at higher temperatures. Possibly this is related to a corresponding behavior reported in the kinematic viscosity η. Experimental data for the $\eta(T)$ in liquid Ge shows a sharp drop just above the melting point, followed by a more gradual decline at higher temperatures.[2] D can be related to η using the Stokes-Einstein relation

$$D = \frac{k_B T}{2 \pi a \eta}, \tag{10}$$

which is quite successful in connecting the two coefficients for a liquid of hard spheres of diameter a. If a is assumed to decrease only slightly with temperature, then a sharp decrease in η is connected to a corresponding increase in D. Thus the sharp rise in D is in qualitative agreement with the experiment for η.

C. Electronic properties

Next, we discuss the electronic density of states $N(E)$ at the same five temperatures. $N(E)$ is calculated from the approximate expression

$$N(E) = \sum_{\mathbf{k}, E_{\mathbf{k}}} w_{\mathbf{k}} g(E - E_{\mathbf{k}}). \tag{11}$$

Here $E(\mathbf{k})$ denotes the energy eigenvalues for the single-particle wave functions at a particular k point of the supercell Brillouin zone and $w_{\mathbf{k}}$ is the weight of that k point (as defined below). $g(E)$ is a Gaussian function of width $\sigma = 0.2$ eV, used in order to give better statistics to the density of states. To carry out the calculation we sampled the supercell Brillouin zone using the set of eight special k points, with equal weights $w_{\mathbf{k}}$, used by Holender *et al.*[29] in their simulation of liquid Ga and we have included the lowest 168 eigenvalues $E_{\mathbf{k}}$ for each $\mathbf{k}$. For each temperature, the final results were then obtained by averaging over five representative configurations in the liquid state.

Figure 10 shows the calculated density of states for $T = 1250$ and 2000 K. At these and all intermediate temperatures, we find that $N(E)$ is finite at the Fermi energy, indicating that liquid Ge is metallic. Another characteristic feature of $N(E)$ is the presence of a pseudogap at -4.6 eV that separates the s-like and p-like bands.[30,31] Even though there is short-range covalent bonding in liquid Ge, this feature is not obviously reflected in the density of states. Furthermore, $N(E)$ does not show any significant temperature variation in the range considered.

Another quantity of interest is the frequency-dependent electrical conductivity $\sigma(\omega)$ and its low-frequency limit, the dc conductivity. $\sigma(\omega)$ can be calculated from the Kubo-Greenwood formula[32]

$$\sigma(\omega) = \frac{2 \pi e^2}{3 m^2 \omega \Omega} \sum_i \sum_j \sum_\alpha (f_j - f_i) |\langle \psi_i | \hat{p}_\alpha | \psi_j \rangle|^2$$

$$\times \delta(E_j - E_i - \hbar \omega). \tag{12}$$

Here m is the electron mass and ψ_i and ψ_j are the single-particle Kohn-Sham wave functions with occupancies f_i and
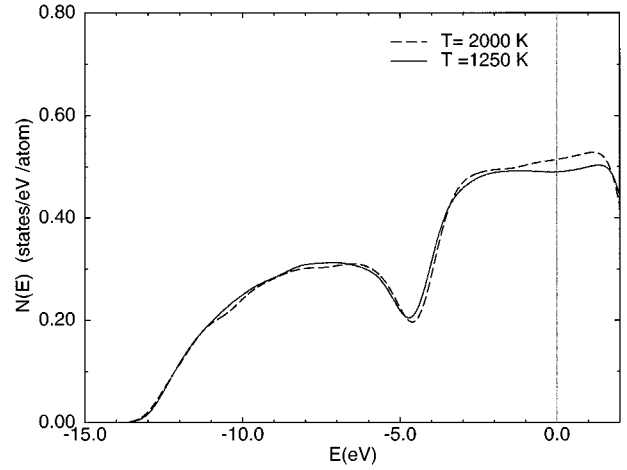

FIG. 10. Calculated electronic density of states $N(E)$ (in states/ eV atom) for liquid Ge at 1250 and 2000 K. Each curve is obtained by averaging over five characteristic atomic configurations; the supercell Brillouin zone is sampled using eight special k points.

f_j and energy eigenvalues E_i and E_j. $\hat{p}_\alpha$ is the component of the momentum operator in the direction α.[33] We have calculated the conductivity using the same set of eight special k points used for $N(E)$ and again averaged over five representative ionic configurations for each temperature. As in the density-of-states calculation, we have included the lowest 168 eigenvalues; the highest of these lies ~ 2.5 eV above the Fermi energy.

The resulting $\sigma(\omega)$ is shown for two temperatures in Fig. 11. At both temperatures, $\sigma(\omega)$ decreases monotonically with ω, showing no absorptive peaks in the observed frequency range. By extrapolating to $\omega = 0$, we estimate the dc conductivity at $T = 1250$ K as 1.5×10^4 $\Omega^{-1} \mathrm{cm}^{-1}$, in good agreement with the measured value of 1.66×10^4 $\Omega^{-1} \mathrm{cm}^{-1}$.[2] The calculated temperature-dependent dc conductivity is shown in Table IV.
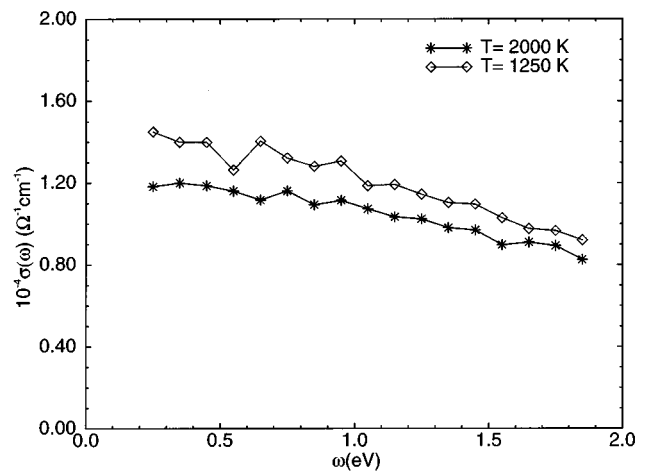

FIG. 11. Calculated ac conductivity $\sigma(\omega)$ for liquid Ge at $T = 1250$ and 2000 K, as obtained by averaging over five typical atomic configurations at each temperature. Line segments merely connect calculated points.

TABLE IV. dc conductivity at the five temperatures obtained by extrapolating low-frequency ac conductivity results.

T (K)	σ_{dc} (10^4 Ω^{-1}cm^{-1})
1250	1.54
1400	1.45
1500	1.42
1600	1.35
2000	1.27

IV. DISCUSSION AND CONCLUSIONS

We now turn to some possible interpretations of the results presented in the preceding section, especially the unusual temperature-dependent structure. It has been argued[34] that the structural properties of liquid metals are basically determined by two length scales: an effective hard-sphere diameter σ, which determines the position of the principal peak in $g(r)$, and the wavelength of Friedel oscillations in the pair potential ($\lambda = \pi/k_F$), where k_F is the Fermi wave vector. This picture has been successfully applied to explain trends in the structural properties of liquid metals.[35] In the following, we use this view to offer some speculations about our own results.

For a simple liquid metal such as Na, the two length scales set by σ and λ are commensurate. Hence, in this picture, the behavior of $g(r)$ can be explained as a consequence of the constraints of hard-sphere packing. But for tetravalent liquid metals, it has been shown[35] that the two length scales are incompatible. In particular, the first maximum of the hard-sphere $g(r)$ coincides with the repulsive part of the effective pairwise interaction. Thus it becomes energetically favorable to shift some atoms from the first shell to a neighboring shell that corresponds to a minimum of the pair potential. This explains the low coordination numbers of tetravalent liquid metals and also the intermediate peak observed in $g(r)$ in both experiment and our simulations, without the necessity of invoking specifically three-body (or bond-angle-dependent) forces. In the static structure factor, this shift is reflected in the appearance of a shoulder at $q = 2k_F$, distinct from the primary peak of $S(q)$ that occurs roughly at $q = 2\pi/\sigma$.

As the temperature increases the following changes take place: (a) because of the increased ionic kinetic energy the effective hard-sphere diameter σ decreases and (b) the lowering of the ionic number density leads to a corresponding decrease in k_F. Thus the two peaks in $S(q)$, corresponding to $2\pi/\sigma$ and $2k_F$, tend to approach each other. The increased thermal disorder also lowers and broadens the first peak in $S(q)$ and makes it broader. These two effects conceivably combine to make shoulder in the $S(q)$ disappear with increasing temperature. In real space, this behavior is reflected in the disappearance or ''flattening'' of the intermediate peak in $g(r)$ and a corresponding broadening of the first peak. As the intermediate maximum disappears, the first shell gains atoms, so that the coordination number increases at higher temperatures.

There are other possible explanations for the shoulder in the structure factor. Three-body forces among the ions, such as those predicted by the pseudopotential theory of interatomic forces in metals, may conceivably produce such a shoulder. A recent paper[36] has shown that a shoulder can be produced by a model in which several Ge ions are assumed to form a single tetrahedral dynamical entity that moves through the liquid as a unit, at least over diffusive time scales. Our calculations, while they do produce the observed shoulder, cannot easily discriminate between these explanations.

Finally, we mention briefly the recent *ab initio* calculations of Stich *et al.*[37] for *l*-Si. These authors find that the explicit inclusion of spin in the density-functional theory tends to enhance the diffusion coefficient in *l*-Si by about 50%. It seems likely, however, that in *l*-Ge, where the degree of covalent bonding is significantly reduced, $D(T)$ should be less influenced than in Si.

In conclusion, we have carried out *ab initio* molecular-dynamics simulations for several properties of *l*-Ge at five different temperatures: 1250, 1400, 1500, 1600, and 2000 K. Our results are in very good agreement with available experimental data. They indicate that liquid Ge is a good metal, but with some special short-range order arising from residual covalent bonding that persists into the liquid state. At the highest temperatures, however, the liquid seems to evolve into a more conventional close-packed liquid metal. Our computed values of the atomic self-diffusion coefficient $D(T)$ are higher than those previously obtained using empirical potentials, but are in good agreement with results from other *ab initio* calculations.

Finally, the present approach suggests a number of possible applications. For example, it can be used to treat the diffusion coefficients of impurities such as Ga and Si in *l*-Ge. The same approach may be useful for treating liquid versions of technologically important compound semiconductors, such as *l*-GaAs and *l*-CdTe, both on and off stoichiometry. The latter materials might be especially worthwhile to study because the electronic structure here should be strongly dependent on both temperature and concentration. While these calculations would be rather demanding computationally, there appear to be few reliable alternatives for treating these rather complicated liquids in a manner that properly includes the electronic structure.

[1] Y. Waseda, *The Structure of Non-Crystalline Materials, Liquids, and Amorphous Solids* (McGraw-Hill, New York, 1980).

[2] V. M. Glazov, S. N. Chizhevskaya, and N. N. Glagoleva, *Liquid Semiconductors* (Plenum, New York, 1969).

[3] T. E. Faber, *Introduction to the Theory of Liquid Metals* (Cambridge University Press, Cambridge, 1972).

[4] M. Shimoji and T. Itami, *Atomic Transport in Liquid Metals* (Trans Tech, Lancaster, PA, 1986).

[5] F. H. Stillinger and T. A. Weber, Phys. Rev. B **31**, 5262 (1985).

[6] J. Q. Broughton and X. P. Li, Phys. Rev. B **35**, 9120 (1987).

[7] A. Arnold, N. Mauser, and J. Hafner, J. Phys. Condens. Matter **1**, 965 (1989).

[8] R. Car and M. Parrinello, Phys. Rev. Lett. **35**, 2471 (1985).

[9] G. Kresse and J. Hafner, Phys. Rev. B **49**, 14 251 (1994).

[10] N. Takeuchi and I. L. Garzón, Phys. Rev. B **50**, 8342 (1994).

[11] V. Godlevsky, J. R. Chelikowsky, and N. Troullier, Phys. Rev. B **52**, 13 281 (1995).

[12] M. J. Gillan, J. Phys. Condens. Matter **1**, 689 (1989).

[13] W. Kohn and L. J. Sham, Phys. Rev. **140**, A1133 (1965).

[14] A. Williams and J. Soler, Bull. Am. Phys. Soc. **32**, 562 (1987).

[15] R. Stumpf and M. Scheffler, Comput. Phys. Commun. **79**, 447 (1994).

[16] M. Bockstedte, A. Kley, and M. Scheffler, Comput. Phys. Commun. (to be published).

[17] J. P. Perdew and A. Zunger, Phys. Rev. B **47**, 558 (1993).

[18] G. B. Bachelet, D. R. Hamann, and M. Schlüter, Phys. Rev. B **26**, 4199 (1982). The generalized norm-conserving pseudopotentials we use are based on the following references: D. R. Hamann, Phys. Rev. B **40**, 2980 (1989); X. Gonze, R. Stumpf, and M. Scheffler, *ibid.* **44**, 8503 (1991).

[19] L. Kleinman and D. M. Bylander, Phys. Rev. Lett. **48**, 1425 (1982).

[20] S. G. Louie, S. Froyen, and M. L. Cohen, Phys. Rev. B **26**, 1738 (1982).

[21] W. Yu, Z. Q. Wang and D. Stroud, Phys. Rev. B **54**, 13 946 (1996).

[22] S. Nosé, J. Chem. Phys. **81**, 511 (1984).

[23] W. G. Hoover, Phys. Rev. A **31**, 1695 (1985).

[24] P. S. Salmon, J. Phys. F **18**, 2345 (1988).

[25] A. Filipponi and A. Di Cicco, Phys. Rev. B **51**, 12 322 (1995).

[26] P. A. Egelstaff, A. C. Duffil, V. Rainey, J. E. Enderby, and D. M. North, Phys. Lett. **31**, 286 (1966).

[27] N. Moll, M. Bockstedte, M. Fuchs, E. Pehlke, and M. Scheffler, Phys. Rev. B **52**, 2550 (1995).

[28] P. V. Pavlov and E. V. Dobrokhotov, Fiz. Tverd. Tela (Leningrad) **12**, 281 (1970) [Sov. Phys. Solid State **12**, 225 (1970)].

[29] J. M. Holender, M. J. Gillan, M. C. Payne, and A. Simpson, Phys. Rev. B **52**, 967 (1995).

[30] W. Jank and J. Hafner, Europhys. Lett. **7**, 623 (1988).

[31] G. Indlekofer, P. Oelhafen, R. Lapka, and H. J. Guntherodt, Z. Phys. Chem. **157**, 465 (1988).

[32] D. J. Thouless, Phys. Rep. **13**, 93 (1974).

[33] Note that the momentum operator, in principle, has contributions arising from the non-locality of the pseudopotential. However, these corrections are typically small, as has been shown by M. Hybertson and S. Louie [Phys. Rev. B **35**, 5602 (1987)] in their calculation of the dielectric constant for solid Ge. We therefore omit these terms from the momentum operator.

[34] J. Hafner and G. Kahl, J. Phys. F **14**, 2259 (1984).

[35] J. Hafner, *From Hamiltonians to Phase Diagrams* (Springer, Berlin, 1987).

[36] N. W. Ashcroft, Nuovo Cimento D **12**, 597 (1990).

[37] I. Stich, M. Parrinello, and J. M. Holender, Phys. Rev. Lett. **76**, 2077 (1996).